A dual effect of ursolic acid to the treatment of multiple sclerosis through both immunomodulation and direct remyelination

Yuan Zhang[a,b,1], Xing Li[a,b,1], Bogoljub Ciric[a], Mark T. Curtis[c], Wan-Jun Chen[d], Abdolmohamad Rostami[a,2], and Guang-Xian Zhang[a,2]

[a]Department of Neurology, Thomas Jefferson University, Philadelphia, PA 19107; [b]Key Laboratory of the Ministry of Education for Medicinal Resources and Natural Pharmaceutical Chemistry, College of Life Sciences, Shaanxi Normal University, Xi'an 710119, China; [c]Department of Pathology, Thomas Jefferson University, Philadelphia, PA 19107; and [d]Mucosal Immunology Section, Oral and Pharyngeal Cancer Branch, National Institute of Dental and Craniofacial Research, National Institutes of Health, Bethesda, MD 20892

Edited by Lawrence Steinman, Stanford University School of Medicine, Stanford, CA, and approved March 9, 2020 (received for review January 6, 2020)

Current multiple sclerosis (MS) medications are mainly immunomodulatory, having little or no effect on neuroregeneration of damaged central nervous system (CNS) tissue; they are thus primarily effective at the acute stage of disease, but much less so at the chronic stage. An MS therapy that has both immunomodulatory and neuroregenerative effects would be highly beneficial. Using multiple in vivo and in vitro strategies, in the present study we demonstrate that ursolic acid (UA), an antiinflammatory natural triterpenoid, also directly promotes oligodendrocyte maturation and CNS myelin repair. Oral treatment with UA significantly decreased disease severity and CNS inflammation and demyelination in experimental autoimmune encephalomyelitis (EAE), an animal model of MS. Importantly, remyelination and neural repair in the CNS were observed even after UA treatment was started on day 60 post immunization when EAE mice had full-blown demyelination and axonal damage. UA treatment also enhanced remyelination in a cuprizone-induced demyelination model in vivo and brain organotypic slice cultures ex vivo and promoted oligodendrocyte maturation in vitro, indicating a direct myelinating capacity. Mechanistically, UA induced promyelinating neurotrophic factor CNTF in astrocytes by peroxisome proliferator-activated receptor γ(PPARγ)/CREB signaling, as well as by up-regulation of myelin-related gene expression during oligodendrocyte maturation via PPARγ activation. Together, our findings demonstrate that UA has significant potential as an oral antiinflammatory and neural repair agent for MS, especially at the chronic-progressive stage.

multiple sclerosis | ursolic acid | immunomodulation | neural repair

Inflammatory demyelination, axonal damage, and neuron loss in the central nervous system (CNS) are hallmarks of the chronic stage of multiple sclerosis (MS) and its animal model, experimental autoimmune encephalomyelitis (EAE) (1, 2). Current MS therapies efficiently inhibit autoimmune response at the early inflammatory (acute) phase, but largely fail to promote myelin repair, especially during the chronic-progressive phase of MS (2). Accumulation of oligodendrocyte progenitor cells (OPCs) is frequently observed in demyelinated lesions of MS patients; however, these cells rarely mature into oligodendrocytes, the myelinating cells in the CNS, resulting in disease progression and failure of spontaneous remyelination (3–5). Thus, a pharmacological intervention that effectively drives OPC maturation in demyelinated lesions, enhancing remyelination, while being at the same time also immunomodulatory, would represent an important advance in MS treatment (3, 6).

Ursolic acid (UA), a triterpenoid compound (molecular weight: 456.7) naturally present in fruit peels and in many herbs and spices, has been widely used as an herbal medicine with a wide spectrum of pharmacological activities (7, 8). UA is a safe (9) and effective treatment in several inflammatory diseases or related experimental models (8, 9), including Parkinson's disease (10), arthritis (11), diabetes (12), and myasthenia gravis (13). UA administration before disease onset also prevents EAE development by inhibiting Th17 cell differentiation (14). In addition, UA has been shown to attenuate neurodegenerative and psychiatric diseases (15). However, the effect of UA treatment on oligodendrocyte development and remyelination in ongoing and chronic EAE is not known.

In the present study, we tested our hypothesis that UA has a dual effect in chronic EAE, immunomodulation, and neuronal repair. We show that EAE severity, CNS inflammation, and demyelination were significantly reversed by UA treatment, even when the treatment was started on day 60 post immunization (p.i.). The direct effect of UA on neural cells and remyelination was then confirmed in a cuprizone-induced demyelination model, a CNS organotypic slice culture system, and oligodendrocyte maturation assays, which, due to their isolation from the systemic immune response, are considered complementary models of neural cell development in the CNS. We further defined a peroxisome proliferator-activated receptor γ (PPARγ)-dependent mechanism of UA action.

Results

Oral UA Effectively Ameliorates CNS Autoimmunity. We first studied whether oral administration of UA has beneficial effects on

Significance

Current immunomodulatory therapies for multiple sclerosis (MS) can effectively inhibit autoimmune response, but largely fail to promote myelin repair. This therapeutic deficiency is due mainly to the failure of treatment to promote remyelination in the central nervous system (CNS). Here we show that ursolic acid (UA), a natural triterpenoid, in addition to its well-known antiinflammatory effect, also directly stimulates oligodendrocyte maturation and CNS myelin repair. Mechanisms of UA action involve induction of pro-myelinating neurotrophic factor in astrocytes by PPARγ/CREB signaling and regulation of myelin-related gene expression during oligodendrocyte maturation via PPARγ activation. Our data demonstrate that UA has great potential as an agent for MS, especially at the chronic-progressive stage, because of its capacity in both immunomodulation and neural repair.

Author contributions: Y.Z., X.L., B.C., A.R., and G.-X.Z. designed research; Y.Z., X.L., M.T.C., and G.-X.Z. performed research; W.-J.C. contributed new reagents/analytic tools; Y.Z., X.L., and M.T.C. analyzed data; and Y.Z., X.L., B.C., W.-J.C., A.R., and G.-X.Z. wrote the paper.

The authors declare no competing interest.

This article is a PNAS Direct Submission.

[1]Y.Z. and X.L. contributed equally to this work.

[2]To whom correspondence may be addressed. Email: a.m.rostami@jefferson.edu or guang-xian.zhang@jefferson.edu.

This article contains supporting information online at https://www.pnas.org/lookup/suppl/doi:10.1073/pnas.2000208117/-/DCSupplemental.

First published April 6, 2020.

ongoing EAE. By administering different doses, we found that 25 mg/kg/d of UA is the optimal dose for suppressing EAE severity (Fig. 1*A*); this dose was therefore used in all subsequent in vivo experiments. UA treatment at this dose also significantly inhibited disease severity when treatment was started at the peak of disease (Fig. 1*B*). UA-treated animals exhibited significantly reduced inflammation and demyelination (Fig. 1 *C* and *D*), as well as a decreased number of mononuclear cells (MNCs) in the CNS compared with the phosphate-buffered saline (PBS)-treated control group (Fig. 1*E*). PBS-treated control mice consistently had a large number of $CD45^+$ leukocyte infiltrates in the demyelinated areas (MBP^-), which was reversed by UA treatment (Fig. 1 *F* and *G*). Furthermore, significantly increased MBP^+ areas and numbers of $CC1^+$ cells (newly matured oligodendrocytes), but reduced density of $A2B5^+$ OPCs in UA-treated mice (Fig. 1 *F* and *G*), suggest that UA induced OPC maturation in CNS lesions. UA administration did not affect expression of the astrocyte marker GFAP (Fig. 1 *F* and *G*). Taken together, these data indicate that UA reduces CNS inflammation and possibly promotes myelin repair by enhancing the maturation of endogenous OPCs into remyelinating oligodendrocytes.

Evaluation of the effect of orally administered UA on the peripheral immune response showed significantly reduced numbers of antigen-presenting cells ($CD11b^+$ and $CD11c^+$) among splenocytes of UA-treated mice and lower expression of costimulatory molecules (*SI Appendix*, Fig. S1*A*). In UA-treated mice, reduced frequencies of IFN-γ^+, IL-17^+, and GM-CSF^+ $CD4^+$ T cells and reduced production of these cytokines in culture were also observed, while there was no effect on Th2/Treg cytokines IL-5 and IL-10 (*SI Appendix*, Fig. S1*B*). In parallel, expression of key transcription factors ROR-γt (Th17 cells) and T-bet (Th1 cells) was significantly reduced in splenocytes isolated from UA-treated EAE mice, while expression of GATA3 (Th2 cells) and Foxp3 (Treg cells) was not affected (*SI*

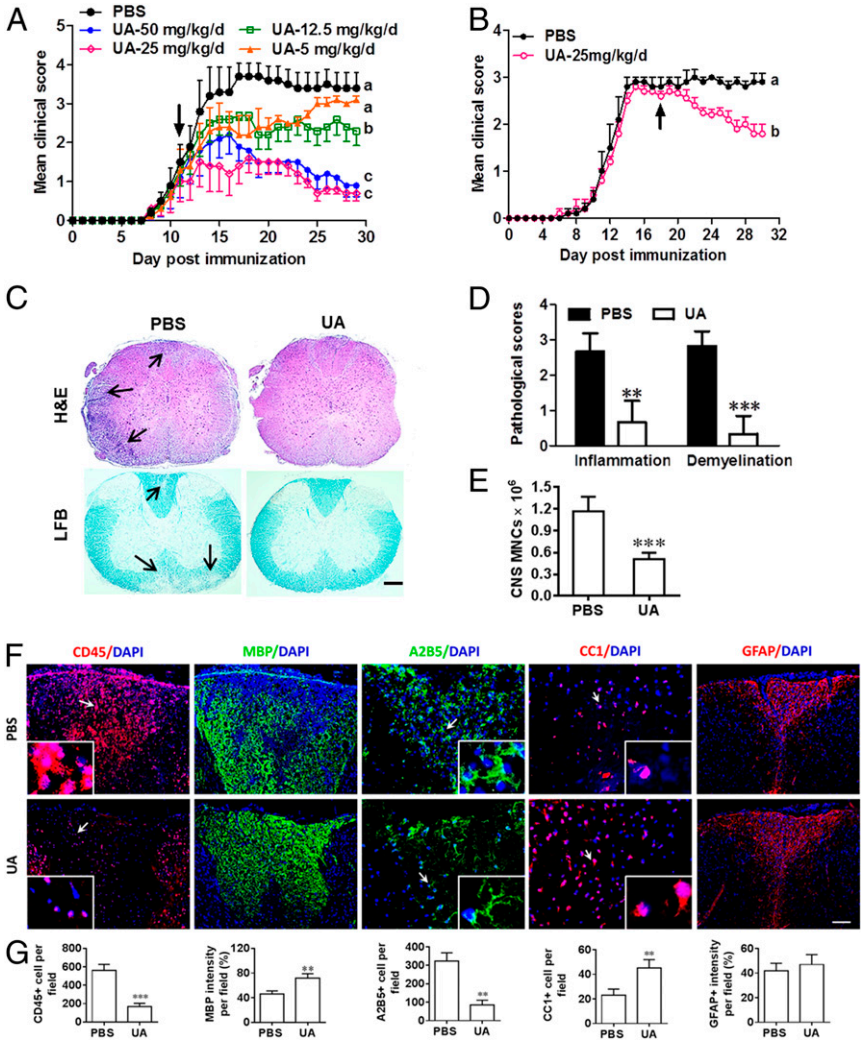

Fig. 1. Oral UA effectively ameliorates acute CNS autoimmunity. Female, 8- to 10-wk-old C57BL/6J mice were immunized with $MOG_{35–55}$ and treated with PBS and different doses of UA (Sigma-Aldrich, St. Louis) by oral gavage daily, starting on day 11 p.i. (onset, *A*) or day 18 p.i. (peak, *B*). Disease was scored daily on a 0 to 5 scale. Thoracic spinal cord sections of EAE mice were analyzed by immunohistochemistry at different stages of the disease before (days 10 and 18 p.i.) or after treatment (day 30 p.i.). (*C*) Sections (lumbar spinal cord) were assayed for inflammation by hematoxylin and eosin (H&E) and demyelination by Luxol fast blue (LFB), and (*D*) CNS pathology was scored on a 0 to 3 scale. (*E*) Absolute number of MNCs in cell suspension of each spinal cord was counted. (*F*) Immunohistochemistry on spinal cord sections of PBS- and UA-treated EAE mice in the dorsal funiculus. Dorsal column at the thoracic spinal cord is shown as representative images. (*G*) Quantitative analysis of CD45, MBP, A2B5, and CC1 expression using Image-Pro. The measured areas included 8 to 10 fields and cover virtually all of the white matter of the spinal cord. Groups designated by the same letter are not significantly different, while those with different letters (a, b, or c) are significantly different, Student's *t* test. $^{**}P < 0.01$, $^{***}P < 0.001$, compared to PBS-treated group, one-way ANOVA with Tukey's multiple comparisons test. All quantifications were made from three independent experiments. Symbols represent mean ± SD; $n = 5$ to 8 mice in each group. (Scale bar, 100 μm in *C*; 40 μm in *F*; and 1 μm in the *Insets*.)

Appendix, Fig. S1*C*). Addition of UA to Th1- and Th17-polarizing cultures inhibited differentiation of these cells in a dose-dependent manner (*SI Appendix*, Fig. S2). These data provide evidence for the immunomodulatory effect of UA in vitro and in vivo.

UA Promotes Neurological Recovery in Chronic EAE. We then determined the therapeutic efficacy of UA in the chronic phase of EAE. This is important, given the unmet need for effective therapies for this stage of MS. When UA treatment (25 mg/kg/d) was initiated at day 60 p.i., at which point chronic myelin and axon damage is already established, clinical disease gradually improved until the mice were killed (Fig. 2*A*). The cumulative score from day 60 to 120 p.i. significantly decreased in the UA-treated group (56.1 ± 3.6) compared to the PBS-treated control (71.5 ± 6.2; $P < 0.05$).

To evaluate the effects of UA on CNS myelin repair at the chronic stage of EAE, immunostaining for myelin and axons was performed within standard 500-μm^2 fields at specific sites of the dorsal column of the lumbar spinal cord (at L3) as CNS demyelinated lesions have been consistently observed in these areas (16). As shown in Fig. 2 *B* and *C*, a significant degree of myelin basic protein (MBP) loss (demyelination) had occurred before treatment at day 60 p.i.; in PBS-treated mice, MBP loss continued to accumulate until day 120 p.i., indicating disease progression. UA-treated mice had smaller demyelinated areas and higher MBP intensity compared to PBS-treated mice (at day 120 p.i. $P < 0.01$). Importantly, at day 120 p.i., the UA-treated group had significantly increased MBP intensity compared to the demyelination baseline (day 60 p.i.; before treatment) (Fig. 2*C*, $P < 0.01$), thus providing evidence that UA treatment not only halts further myelin damage, but also promotes myelin recovery.

We then determined the effect of UA on axonal loss within spinal cord lesions using anti-MBP (myelin marker) and anti-neurofilament (NFH; axonal marker) staining. As shown in Fig. 2 *B–E*, apparent demyelination (NFH$^+$MBP$^-$), as well as axon and myelin loss (NFH$^-$MBP$^-$), were observed at day 60 p.i. (before treatment), and significantly fewer myelinated axons (NFH$^+$MBP$^+$) were found at day 120 p.i. in PBS-treated mice, indicating disease progression. In regions of myelin loss (MBP low or negative), NFH staining showed fiber deterioration and reduced axon numbers, indicative of the axonal pathology that accompanies the demyelination process. In contrast, mice treated with UA had a significantly greater number of axons, especially myelinated axons (NFH$^+$; red) surrounded by MBP$^+$ rings (green), indicating the beneficial effects of UA in axonal protection and repair. Importantly, the high magnification fields of Fig. 2*B* are from the upper regions of the dorsal columns, which are constituted mainly of ascending sensory fibers from dorsal root ganglion (DRG) neurons. Therefore, the increased number of axons in that region of the dorsal columns reflects, at least in part, the axonal sprouting from those DRG neurons.

Furthermore, ultrastructural analyses of ventral spinal cords revealed increased myelinated/remyelinated axons in lesions of UA-treated mice compared to controls, and the fairly large size of the axons suggests that they may be descending corticospinal tract axons that directly contact motor neuron perikarya. Quantitative analysis confirmed that there were more remyelinated axons in UA-treated mice, as determined by greater numbers of axons surrounded by thinner-than-normal myelin (Fig. 2*G*).

Given the neuronal abnormalities, e.g., dendrite disruption and perikaryal atrophy, at the chronic stage of EAE (16), and the protective effect of UA on neurons (10, 17, 18), we further evaluated neuronal pathology after UA treatment using microtubule-associated protein 2 (MAP2) immunostaining at the lumbar anterior horns. MAP2 is specifically expressed in dendrites and plays a key role in dendritic outgrowth, branching, and synaptogenesis. Consistent with a previous study (16), PBS-treated EAE mice exhibited dendritic abnormalities (thinning, shortening, fragmentation, and even loss) and neuron perikaryal atrophy. These neuronal abnormalities were significantly decreased after UA treatment, and MAP2a$^+$ perikarya remained similar to those in naive mice, which most likely indicates dendritic regeneration of motor neurons (Fig. 2 *H* and *I*).

Taken together, these results clearly demonstrate the reparative capacities of oral UA for damaged myelin, axons, and neurons.

The Therapeutic Effect of UA on EAE Is PPARγ Dependent. Given that UA functions as an agonist of PPARγ (19), the activation of which mitigates neuroinflammation and exerts direct neuronal protection after CNS injuries (20), we first confirmed the structural basis and binding affinity of UA to PPARγ using molecular docking (*SI Appendix*, Fig. S3). The crystal structure of PPARγ (Protein Data Bank code: 2Q5S) bound to the synthetic ligands thiazolidinedions was used (https://www.rcsb.org/structure/2Q5S). From the generated docking model, UA was located in the binding pocket of PPARγ (*SI Appendix*, Fig. S3*A*), and a hydrogen bond formed between oxygen in the carboxyl group and Glu343 (*SI Appendix*, Fig. S3*B*). The role of PPARγ in the suppressive effect of UA on EAE was then tested in PPARγ-deficient heterozygous mice (PPARγ$^{+/-}$), as PPARγ knockout is embryonically lethal (20). As shown in Fig. 3*A*, the PPARγ$^{+/-}$ mice developed EAE with prolonged clinical paralysis similar to the wild-type (WT) littermates (PPARγ$^{+/+}$); however, oral UA did not protect PPARγ$^{+/-}$ mice from EAE even in the prophylactic regimen (administration starting from day 0 p.i.). In line with the clinical scores, UA decreased CNS inflammation and demyelination and promoted MBP expression in WT, but not in PPARγ$^{+/-}$ mice (Fig. 3 *B* and *C*). These results suggest that the mitigating effect of UA in CNS autoimmunity is PPARγ dependent.

UA Enhances Remyelination in Cuprizone-Induced Demyelination in a PPARγ-Dependent Manner. Neurologic recovery in EAE mice treated with UA might be secondary to its immunomodulatory effects. To test the direct myelinating effect of UA, we used the toxic cuprizone-induced demyelination model with minimal inflammatory and T cell-dependent components (21). Wild-type mice were fed with cuprizone for 6 wk to achieve complete demyelination in the corpus callosum; cuprizone was then withdrawn and mice were again fed normal chow, allowing for spontaneous remyelination to take place within the next 2 wk. Upon withdrawal of cuprizone, UA treatment was initiated to specifically determine its effect on the remyelination process (Fig. 4*A*). Under a 6-wk cuprizone treatment, most of the axons in the corpus callosum lost their myelin sheath while there were a few axons with loosely wrapped myelin, as evaluated by ultrastructual electron microscopy (EM) (Fig. 4*B*). Two weeks after cuprizone withdrawal, spontaneous remyelination was observed in the PBS-treated group, while UA treatment significantly reduced the G-ratio of the remyelinated axons, indicating a better recovery from demyelination (Fig. 4 *B–D*). These findings suggest that UA treatment facilitates remyelination in the cuprizone-induced demyelination model.

We also examined the role of PPARγ in UA-induced remyelination in the cuprizone model. In agreement with our findings described above, the postcuprizone recovery of mature myelin in the body of the corpus callosum of WT mice, but not in PPARγ$^{+/-}$ mice, was remarkably accelerated (2.5- to 4-fold increase) by UA supplementation (Fig. 4 *E* and *F*). UA supplementation following cuprizone withdrawal dramatically increased CC1$^+$ oligodendrocyte numbers (3.6-fold), but led to an ∼60 and ∼67% reduction in IBA1$^+$ microglial cells and A2B5$^+$ OPCs,

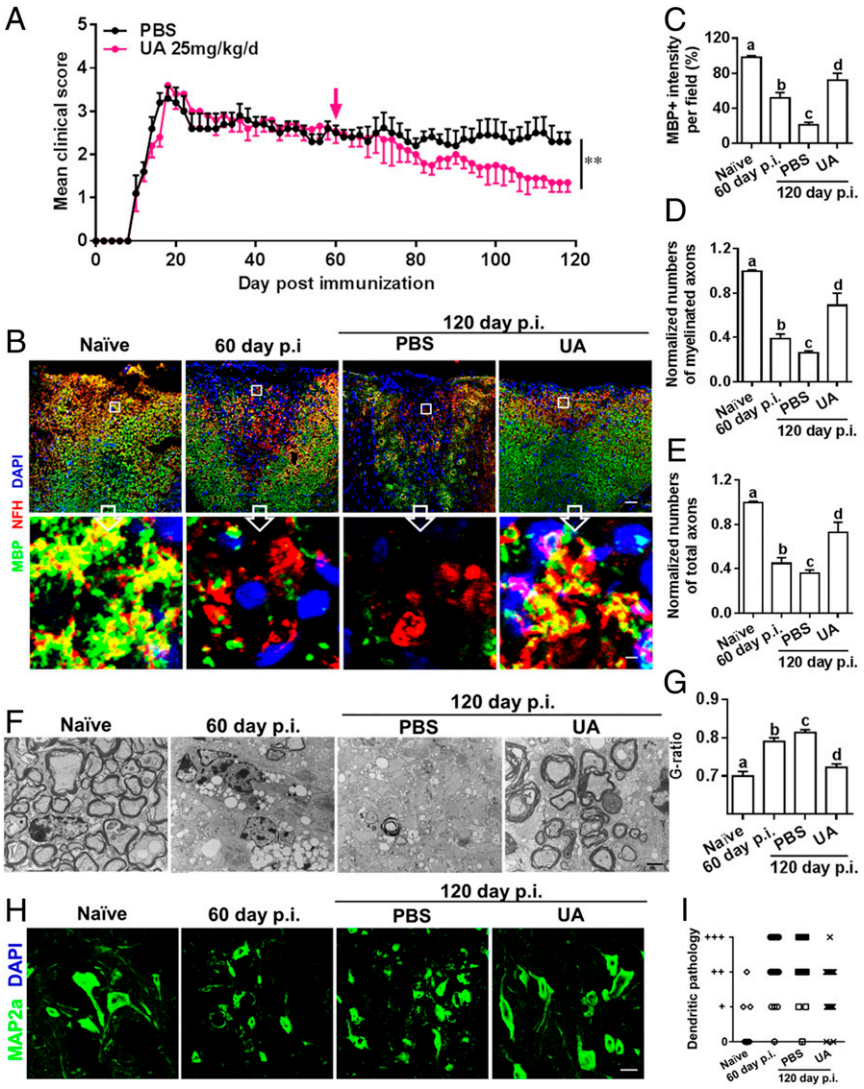

Fig. 2. UA treatment alleviates chronic EAE, promotes remyelination, and reduces axon degeneration and neuron dendrite disruption. Female, 8- to 10-wk-old C57BL/6J mice were immunized with $MOG_{35–55}$ and treated with PBS or UA (25 mg/kg/d) by oral gavage daily, starting on day 60 p.i. (late stage of chronic EAE). (*A*) Disease was scored daily on a 0 to 5 scale (mean ± SD; $n = 6$ to 10 each group). Lumbar spinal cords of naive and EAE mice were harvested before (day 60 p.i.) or after treatment (day 120 p.i.). (*B*) Double immunostaining of MBP (green) and NFH (red; for axons) showing significantly increased numbers of myelinated axons in the dorsal column of the spinal cord (MBP^+NFH^+). (Scale bar, 20 μm for the *Upper* row, and 1 μm for the *Insets* in the *Lower* row). (*C*) MBP intensity was measured in the white matter of spinal cord using Image-Pro. (*D*) Quantification of myelinated axons (MBP^+NFH^+) using Image-Pro. (*E*) Total axons (NFH^+) were quantified using Image-Pro. (*F*) Electron micrographs for tissues of ventral lumbar spinal cords of PBS- and UA-treated EAE mice. (Scale bar, 2 μm.) (*G*) Quantification of the G-ratio (axon diameter/fiber diameter) of myelinated fibers in the ventral lumbar spinal cords of vehicle- and UA-treated EAE mice (PBS group, G-ratio = 0.8136 ± 0.006856; UA group, G-ratio = 0.7225 ± 0.008690). (*H*) MAP2a (green; dendrite marker) immunostaining at lumbar anterior horns of PBS- and UA-treated mice. (Scale bar, 10 μm.) (*I*) Scoring of $MAP2a^+$ neuron dendritic disruption of different groups following a previously described protocol (16). A score of 0 (normal) was assigned when most or all neuron dendrites were of normal thickness and length. A score of "+" was assigned when the majority of neuron dendrites were thinner than normal, a score of "++" when the majority of neuron dendrites were shortened or fragmented, and a score of "+++" when the majority of neuron dendrites were lost. Groups designated by the same letter are not significantly different, while those with different letters (a, b, c, or d) are significantly different ($P < 0.05$ to 0.01), one-way ANOVA with Tukey's multiple comparisons test. $^{**}P < 0.01$, compared to PBS-treated group, one-way ANOVA with Tukey's multiple comparisons test. All quantifications were made in three independent experiments. Symbols represent mean ± SD; $n = 10$ random areas per group.

respectively (Fig. 4 *G* and *H*), suggesting that UA reduced microglia activation, as well as induced OPC maturation in the demyelinated lesions of the corpus callosum. However, the remyelination process and microgliosis were unaltered by UA in $PPAR\gamma^{+/-}$ mice, similar to what we found in EAE mice. Also, UA administration did not impact expression of the astrocyte marker GFAP in either WT or $PPAR\gamma^{+/-}$ mice (Fig. 4 *G* and *H*). Overall, UA supplementation supports oligodendrocyte differentiation, promotes remyelination, and attenuates axonal damage after cuprizone withdrawal, and these effects of UA treatment are PPARγ dependent.

UA Enhances Remyelination in Organotypic Cerebellar Slices. We then investigated the remyelinating effect of UA in another, completely distinct ex vivo model, lysophosphatidylcholine (LPC)-induced demyelination in organotypic cerebellar slices. At day 2 post LPC treatment, a notable decrease in myelinated axons, as determined by the colocalization of MBP and NFH

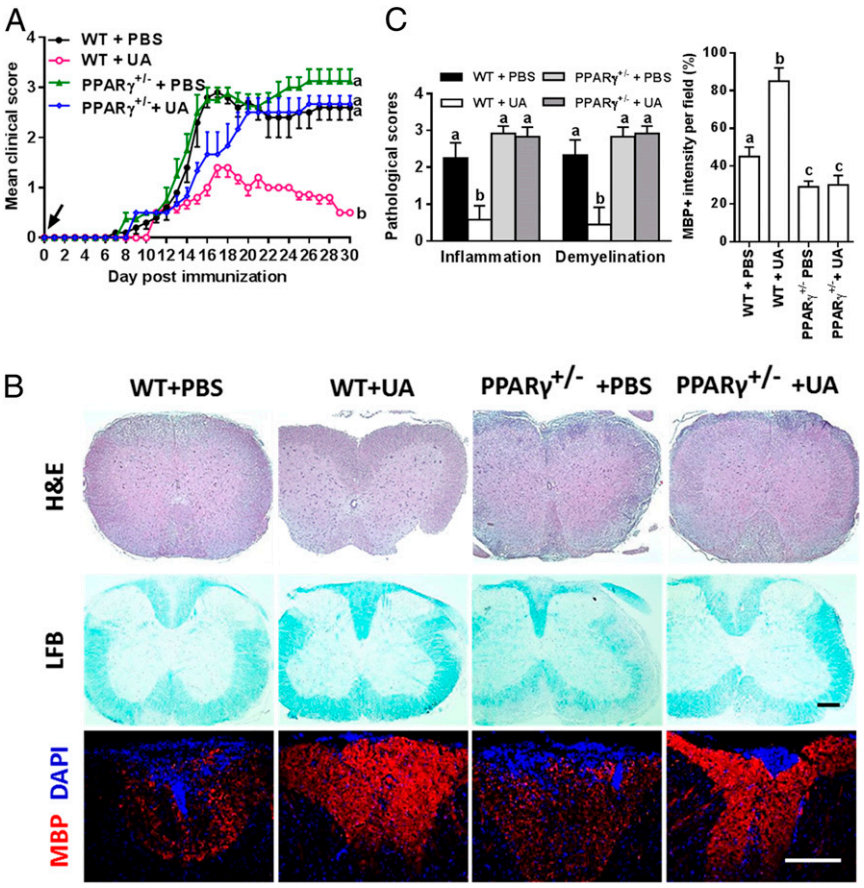

Fig. 3. The therapeutic effect of UA on CNS autoimmunity is PPARγ dependent. (*A*) Clinical score of UA- or PBS-treated WT ($PPAR\gamma^{+/+}$) or $PPAR\gamma^{+/-}$ mice (C57BL/6J background). (*B*) Sections (lumbar) were assayed for inflammation by H&E, demyelination by LFB, and MBP expression by immunostaining. Dorsal column at the thoracic spinal cord is shown as representative images. (*C*) CNS pathology was scored on a 0 to 3 scale, and MBP intensity was measured in the white matter of spinal cord using Image-Pro. The measured areas included 8 to 10 fields and covered virtually all of the white matter of the spinal cord. Groups designated by the same letter are not significantly different, while those with different letters (a, b, or c) are significantly different ($P < 0.05$–0.01). All quantifications were made from three independent experiments. Symbols represent mean ± SD; $n = 5$ to 8 mice per group. (Scale bar, 100 μm in *B*.)

staining, was observed in the UA-treated (LPC + UA) and untreated (LPC) groups compared with the normally myelinated group (PBS) (Fig. 5 *A* and *B*; both $P < 0.001$). A certain spontaneous recovery of MBP expression and ensheathment occurred at day 14 post LPC treatment (4.6- ± 1.3-fold compared with day 2 post LPC treatment; Fig. 4*B*); however, remyelination was incomplete at this time point as shown previously (22). After 14 d of treatment (LPC + UA), a significant increase in myelinated axons was observed compared to the control group (2.1- ± 0.2-fold over LPC control, $P < 0.001$), indicating enhanced remyelination by UA (Fig. 5*B*).

We then examined the effects of UA on the expression of several cytokines and neurotrophin in organotypic slice cultures (at day 14 post LPC and UA treatment), which included a total of 37 neurotrophin genes in the neurotrophin and receptor PCR array and 8 cytokine genes. Ten genes were down-regulated and 19 were up-regulated. UA treatment substantially reduced expression of inflammatory factors, including TNFα, iNOS, and GM-CSF, while enhancing expression of several antiinflammatory cytokines. Among neurotrophins tested, the most robustly induced (~50-fold higher over LPC control) was ciliary neurotrophic factor (CNTF; Fig. 5*C*), an important survival factor for oligodendrocytes, with a strong myelinating effect (23). Other neurotrophic factors up-regulated by UA treatment included brain-derived neurotrophic factor, fibroblast growth factor, glial cell line-derived neurotrophic factor, glia maturation factor, and nerve growth factor, but with much lower levels than CNTF (also in Fig. 5*C*). The induction of CNTF was further verified by an enzyme-linked immunosorbent assay (ELISA) (3.9- ± 0.8-fold over LPC control, $P < 0.001$; Fig. 5*D*). Collectively, UA treatment significantly promoted remyelination in an LPC-induced demyelination model, most likely through creating a supportive environment, e.g., induction of neurotrophic factor CNTF.

CNTF Secreted by UA-Treated Astrocytes Enhanced OPC Maturation In Vitro. Given that CNTF was the most robustly induced by UA among all neurotrophic factors tested (as discussed above for Fig. 5*C*) and that astrocytes are the main source of CNTF (24), we first examined if UA could stimulate CNTF expression in astrocytes in vivo in EAE mice when treatment was started at day 60 p.i. Whereas almost no CNTF staining was found in $GFAP^+$ cells in PBS-treated EAE mice, a remarkable elevation of CNTF-positive staining was found to colocalize with $GFAP^+$ cells in UA-treated EAE mice (Fig. 6 *A* and *B*). In vitro, UA induced up to a 25-fold increase in CNTF messenger RNA (mRNA) expression in primary astrocytes, while induction of other CNTF family members, e.g., IGF1, IL-11, and leukemia inhibitory factor (LIF), was much lower (Fig. 6*C*). Consistent with increased mRNA levels, CNTF protein concentrations were significantly elevated in the supernatants of cultured astrocytes after UA treatment (Fig. 6*D*).

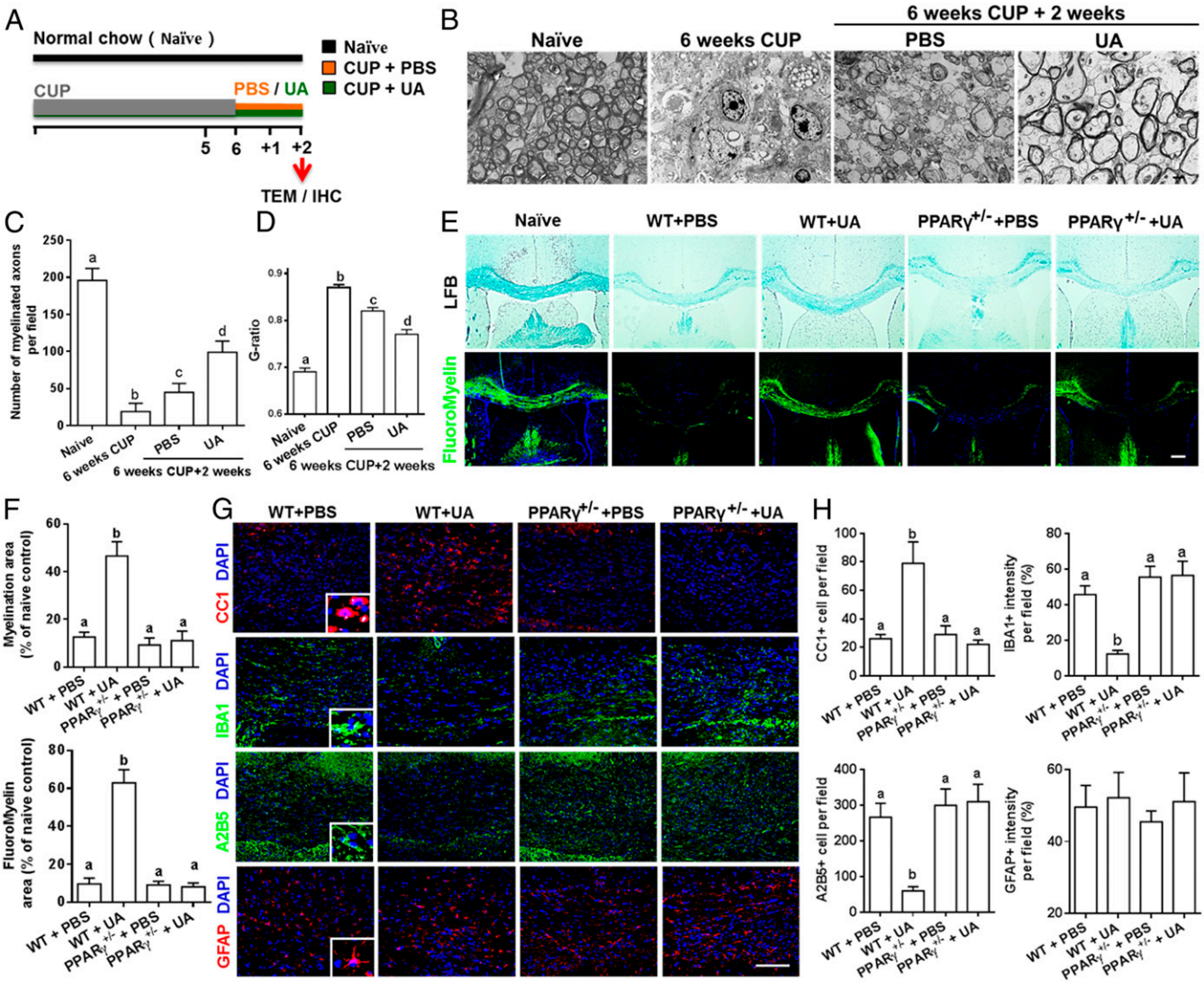

Fig. 4. UA enhances remyelination in cuprizone-induced demyelination in a PPARγ-dependent manner. (*A*) Treatment paradigms. Male, 8- to 10-wk-old C57BL/6J mice were fed with cuprizone (CUP) for 6 wk to achieve complete demyelination, followed by feeding PBS or UA (25 mg/kg/d) for another 2 wk. (*B*) Representative electron microscopy images of the corpus callosum region isolated from cuprizone-fed mice treated with UA or PBS for 2 wk. (*C*) Quantification of the myelinated axons. (*D*) Quantification of the G-ratios (axon diameter/fiber diameter) of myelinated fibers. (*E*) Representative LFB and FluoroMyelin stains in the body of the corpus callosum of UA- or PBS-treated WT or PPARγ$^{+/-}$ mice at 2 wk after cuprizone withdrawal. (*F*) Quantitative analysis of myelinated and fluoromyelinated areas measured in the body of the corpus callosum using Image Pro software. (*G*) Immunohistochemistry on corpus callosum sections of UA- or PBS-treated WT or PPARγ$^{+/-}$ mice at 2 wk after cuprizone withdrawal. (*H*) Quantitative analysis of GFAP, IBA1, A2B5, and CC1 expression using Image-Pro. Groups designated by the same letter are not significantly different, while those with different letters (a, b, c, or d) are significantly different ($P < 0.05$ to 0.01), one-way ANOVA with Tukey's multiple comparisons test. All quantifications were made from three independent experiments. Symbols represent mean ± SD; $n = 5$ to 8 mice each group. (Scale bar, 2 μm in *B*, 100 μm in *E*, and 20 μm in *G*.)

To confirm that CNTF secreted by UA-treated astrocytes has a role in OPC maturation, we treated primary OPCs with astrocyte-conditioned media (UA-ACM). As shown in Fig. 6*E*, OPCs treated with UA-ACM for 7 d became mature MBP^{+} oligodendrocytes with more myelin sheaths and branching of the processes compared with those treated with PBS-ACM, and these effects were abolished by the presence of CNTF-neutralizing antibody (Fig. 6 *E* and *F*). These results indicate that CNTF secreted by UA-treated astrocytes contributes to oligodendrocyte maturation.

UA Induced Astroglial CNTF Production through PPARγ/CREB Signaling. Given that UA functions as an agonist of PPARγ (*SI Appendix*, Fig. S3) to promote remyelination (Figs. 3 and 4), we then investigated whether UA induces astroglial CNTF expression via PPARγ. We first investigated the role of PPARγ signaling in astrocytes during EAE by its knockdown in astrocytes as described in our previous study (25). Consistent with the observations in PPARγ$^{+/-}$ mice with EAE, LV-GFAPpro-shPPARγ treatment significantly blocked the mitigating effects of UA in disease progression, as indicated by unaltered disease scores and failure to recover (*SI Appendix*, Fig. S4*B*). Both PPARγ and CNTF expression levels in GFP^{+} astrocytes from LV-GFAPpro-shPPARγ–treated mice were significantly downregulated compared with those from LV-GFAPpro-shCtrl–treated mice (*SI Appendix*, Fig. S4*C*). Although CNTF expression was obviously induced in sorted astrocytes by UA in LV-GFAPpro-shCtrl –treated EAE mice, this effect was significantly blocked in LV-GFAPpro-shPPARγ–treated EAE mice (*SI Appendix*, Fig. S4*C*).

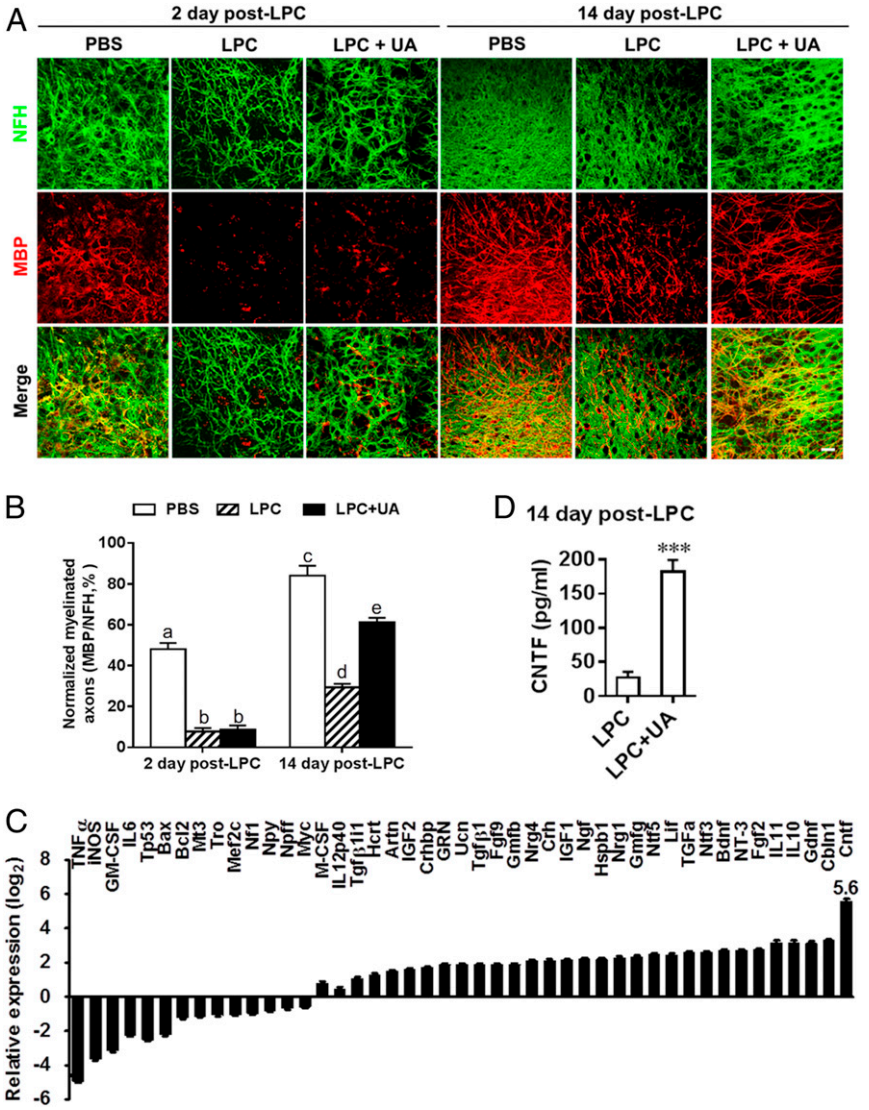

Fig. 5. UA enhances remyelination following LPC demyelination of organotypic cerebellar slices. Cerebellar slices from postnatal day 1 to 2 mouse pups were cultured for 6 d and then demyelinated using LPC for 16 h. Cultures were then allowed to remyelinate over the next 2 or 14 d in the presence or absence of UA (10 μg/mL), after which remyelination was assessed using specific antibodies. (*A*) Representative confocal images of slices at days 2 and 14 post LPC-induced demyelination, immunostained against axons (NFH; green) and myelin (MBP; red). (Scale bar, 20 μm.) (*B*) Quantification of myelinated axons by the alignment of axonal and myelin markers. (*C*) Expression of neurotrophin genes of organotypic slice cultures treated with vehicle (LPC group) or UA (LPC + UA group) at day 14 post LPC was determined using Custom RT^2 Profiler PCR Array (Qiagen, Valencia, CA). (*D*) Supernatants of organotypic slice cultures treated with vehicle (LPC group) or UA (10 μg/mL, LPC + UA group) at day 14 post LPC were analyzed by ELISA for the level of CNTF. Data are shown as mean values ± SD ($n = 5$ to 6 per group) and are representative of three experiments. Groups designated by the same letter are not significantly different, while those with different letters are significantly different ($P < 0.05$ to 0.001), ***$P < 0.001$, compared to untreated group, one-way ANOVA with Tukey's multiple comparisons test.

These data indicate that the improvement brought about by UA treatment in EAE mice is mediated, at least partially, by astroglial PPARγ signaling.

Next, to investigate the mechanism underlying UA-mediated up-regulation of astroglial CNTF via PPARγ, primary astrocytes were incubated with UA and/or specific antagonists for PPARγ, and CNTF production was then determined by immunofluorescence analysis (*SI Appendix*, Fig. S4*D*). CNTF expression was highly induced in astrocytes by UA, and this induction was largely abrogated by the PPARγ-specific antagonist GW-9662 (*SI Appendix*, Fig. S4 *D* and *E*). These results indicate that PPARγ-dependent signals mediate the effect of UA on CNTF protein expression. We then further tested whether UA induced PPAR activity in astrocytes using peroxisome proliferator elements (PPRE)-luciferase reporter assay (26). Primary mouse astrocytes were transfected with tk-PPRE ×3-Luc, a PPRE-dependent luciferase construct, and luciferase activity was then measured. PPAR-specific agonist (WY-14643) was used as positive control. As shown in Fig. 7*A*, UA alone was able to induce PPRE-dependent luciferase activity in a dose-dependent manner, indicating a direct and strong capacity of UA for PPAR activation in astrocytes.

In addition, we investigated mechanisms by which PPARγ controls UA-induced CNTF expression in astrocytes. Surprisingly, using the MatInspector promoter analysis tool (Genomatix software GmbH), we found that the CNTF promoter does not contain any PPREs for PPARs to bind, ruling out a direct role of PPARs in regulating CNTF expression. Rather, the promoter

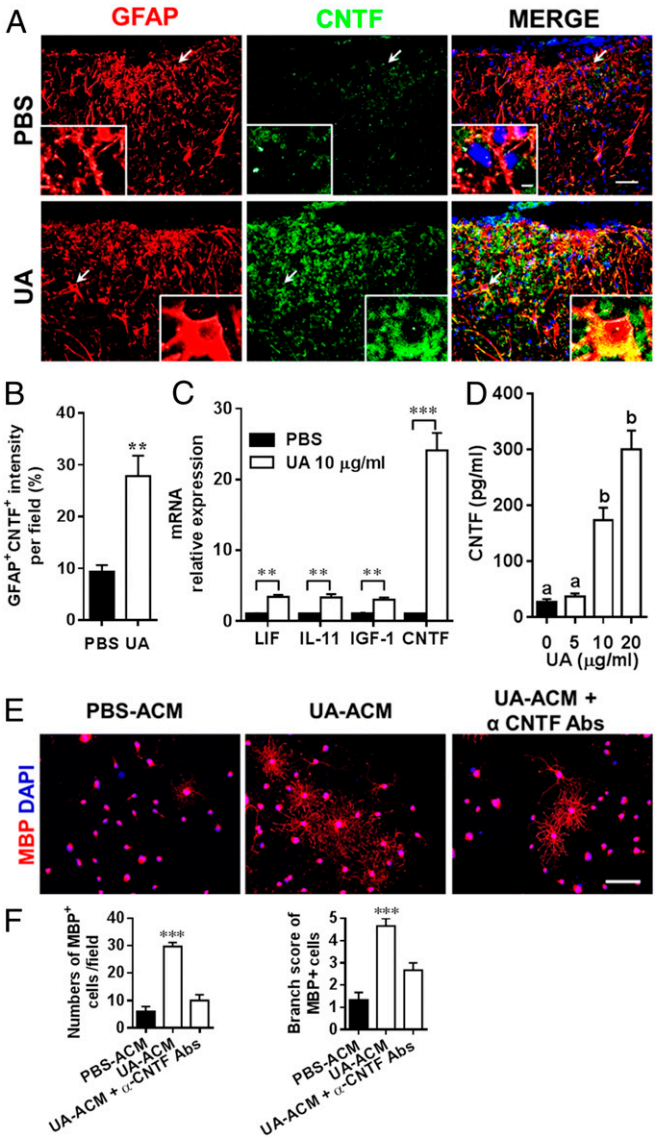

Fig. 6. CNTF secreted by UA-treated astrocytes enhances OPC differentiation in vitro. EAE mice were treated with UA or PBS as shown in Fig. 3*A*. (*A*) Thoracic spinal cord sections of EAE mice were analyzed by double immunostaining of GFAP (red) and CNTF (green). (Arrows indicated the area of the inset. Scale bar, 20 μm.) (*B*) GFAP$^+$ and CNTF$^+$ intensity was measured in the white matter of spinal cord using Image-Pro. (*C*) Primary mouse astrocytes isolated from 2- to 3-d-old pups were cultured in six-well cell culture plates or glass slide chambers. After 24 h, cells were treated with UA at indicated concentrations. mRNA relative expression of LIF, IL-11, IGF1, and CNTF in astrocytes treated with UA (10 μg/mL) for 6 h was detected by real-time PCR. (*D*) After 72 h of UA treatment, the protein level of CNTF in the supernatants was assayed by ELISA. (*E*) Supernatants from UA-treated astrocytes enhanced OPC differentiation. OPCs (5,000 cells/cm^2) were cultured in differentiation medium for 3 d, and half of the medium was replaced by culture supernatants (astrocyte-conditioned media) of astrocytes treated with UA (UA-ACM) or PBS (PBS-ACM) in the presence or absence of CNTF-neutralizing antibodies (α-CNTF-Abs) for another 4 d. Mature oligodendrocytes are identified by the specific marker MBP (red). (Scale bar, 50 μm.) One of five representative experiments is shown. (*F*) Quantitative analysis was performed for numbers or branch score of MBP$^+$ mature oligodendrocytes. Data are shown as mean values ± SD ($n = 5$ to 6 per group) and are representative of three independent experiments. Groups designated by the same letter are not significantly different, while those with different letters are significantly different ($P < 0.05$–0.001). $^{**}P < 0.01$, $^{***}P < 0.001$, compared to control group, one-way ANOVA with Tukey's multiple comparisons test.

harbors multiple cAMP response elements (CRE) for CREB. CREB, the promoter of which does contain a consensus PPRE site (−1,164 to −1,152), is directly activated by PPARα/γ at the transcriptional level in neurons as well as in astrocytes (27, 28). We therefore hypothesized that UA-induced CNTF expression is regulated by PPARγ via CREB. To test this hypothesis, we performed site-directed mutagenesis of the PPRE in the CREB promoter (Fig. 7*B*). The mutant and wild-type promoter constructs pCREB(mut) and pCREB(wt) were then cloned into the pGL4.20 vector and transfected into mouse primary astrocytes. UA treatment markedly induced pCREB(wt)-driven luciferase activity in astrocytes (Fig. 7*C*). Suppression of pCREB(wt) luciferase activity in UA-treated astrocytes by GW-9662, an antagonist of PPARγ, suggested that PPARγ plays a role in UA-induced activation of the CREB promoter. Furthermore, when the construct with the mutated PPRE site pCREB(mut) was transfected into mouse primary astrocytes, we found a dramatic decrease in luciferase activity in UA-treated cells containing the mutant construct (Fig. 7*C*).

A causal relationship between UA-mediated CREB induction and CNTF expression was also verified by knockdown experiments. Astrocytes were treated with lentivirus-delivered CREB-specific small interfering RNA (siRNA) (LV-siCREB), followed by the addition of UA. Successful knockdown of CREB expression (Fig. 7*D*), which resulted in decreased CNTF expression in astrocytes, was confirmed. Notably, induction of CNTF by UA was abrogated after CREB knockdown, as shown by immunofluorescence analysis (Fig. 7 *E* and *F*). Taken together, these findings provide evidence that UA induces CNTF expression in astrocytes via PPARγ/CREB signaling.

UA Directly Induces OPC Maturation via PPARγ Signaling. To examine whether UA has a direct effect on OPC maturation, we analyzed the effects of UA on primary OPC cultures. Under differentiation conditions, UA treatment enhanced OPC maturation into mature oligodendrocytes, with myelin-like sheaths and extension of processes in a dose-dependent manner (Fig. 8 *A*–*C*). Consistent with these findings, UA treatment down-regulated the expression of OPC-specific transcription factors (e.g., Olig2, Nkx2.2) and cell-surface markers (e.g., PDGFRα, NG2) with up-regulated mRNA expression of classic and defining markers of bona fide oligodendrocytes such as Mag, Mog, Cnp1, Plp1, and Mbp (Fig. 8*D*).

We next investigated the role of PPARs in UA-mediated myelin gene expression and maturation of primary OPC cultures. Immunofluorescence analysis showed a significant increase in numbers of MBP$^+$ oligodendrocytes (Fig. 8 *E* and *F*) and morphological changes (Fig. 8 *E* and *G*) under UA treatment; however, this effect was abrogated by GW-9662, a PPARγ-specific antagonist (Fig. 8 *E*–*G*), indicating that UA-induced OPC maturation was PPARγ dependent. As PPARs are known to bind PPREs present in the promoters of different genes, we searched the promoter regions of up-regulated oligodendrocyte genes shown in Fig. 8*D* using the MatInspector promoter analysis tool and PPRESearch (http://www.classicrus.com/PPRE/). The results showed that Cnp1 and Klk6 promoters harbor consensus PPREs (Fig. 8*H*), and UA-induced Cnp1 and Klk6 production was blocked by the PPAR-γ antagonist GW-9662 (Fig. 8 *I* and *J*). Together, our results indicate that UA also acts as a potent promyelinating compound, directly inducing OPC maturation via the PPARγ-signaling pathway.

Discussion

Given the chronic inflammation and extensive tissue damage in the CNS at the chronic stage of MS/EAE, an ideal therapeutic strategy would have the capacity both to suppress CNS

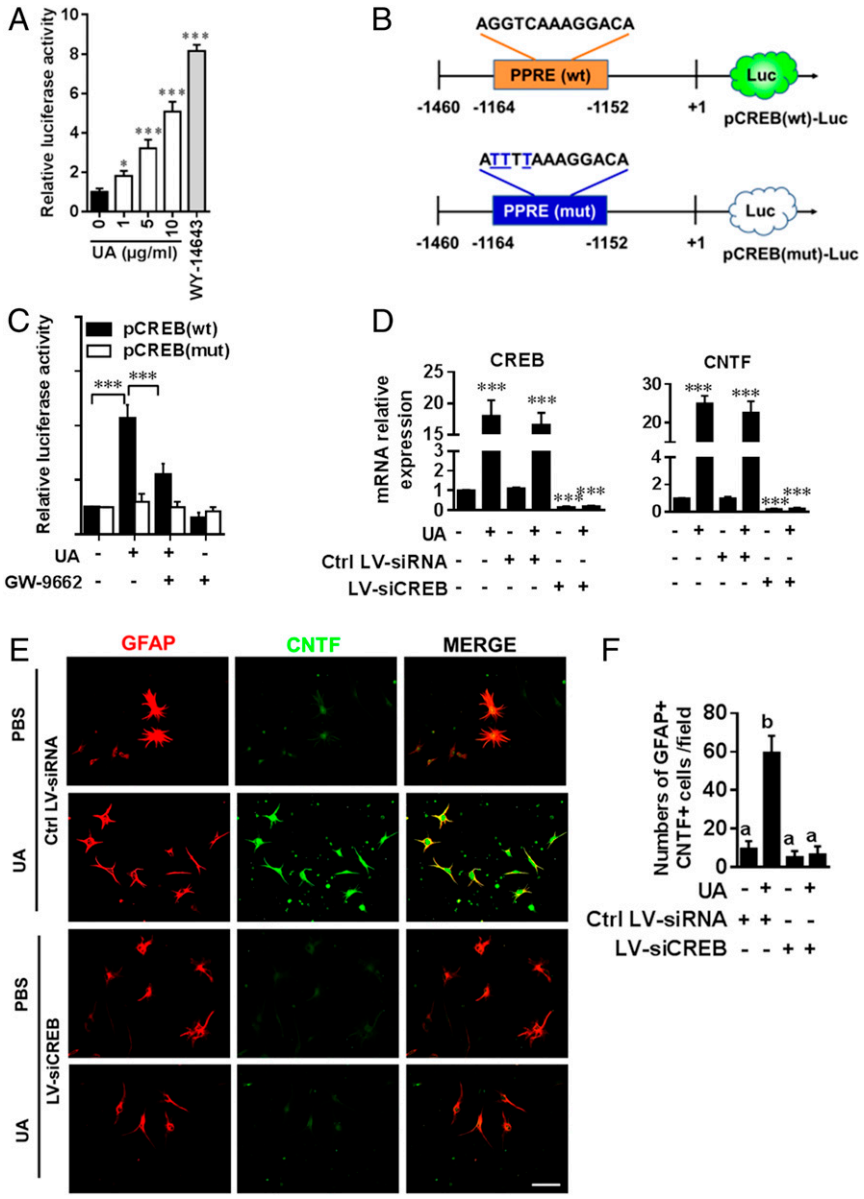

Fig. 7. UA induces astroglial CNTF production via PPARγ/CREB signaling. (*A*) Astrocytes were transfected with tk-PPRE ×3-Luc (Addgene plasmid #1015), a PPRE-dependent luciferase reporter construct. pRLTK, a plasmid encoding Renilla luciferase, was used as transfection efficiency control. After 24 h of transfection, cells were cultured with different concentrations of UA (0, 1, 5, and 10 μg/mL) for 6 h, and activity of firefly and Renilla luciferase was monitored in cell lysates by a Dual-Glo Luciferase Assay kit (Promaga). Data were normalized to an internal control Renilla luciferase ($n = 8$). (*B*) Map of wild-type and mutated CREB promoter constructs. (*C*) Astrocytes were transfected with pCREB(mut) and pCREB(wt) for 24 h followed by treatment with UA (10 μg/mL) or GW-9662 (10 nM) alone and in combination and subjected to luciferase assay. (*D*) CREB and CNTF expression in astrocytes transfected with CREB-specific or control LV-siRNAs overnight in the presence or absence of UA (10 μg/mL) was detected by real-time PCR. (*E*) Primary mouse astrocytes isolated from 2- to 3-d-old pups were cultured in glass slide chambers. Double labeling of astrocytes for GFAP and CNTF was performed under indicated treatment: PBS, UA (10 μg/mL) or UA + LV-siCREB/LV-siRNA. (Scale bar, 50 μm.) One of five representative experiments is shown. (*F*) Quantitative analysis was performed for numbers of $GFAP^+CNTF^+$ cells. Data are shown as mean values ± SD ($n = 5$ to 6 per group) and are representative of three experiments. Groups designated by the same letter are not significantly different, while those with different letters are significantly different ($P < 0.05$ to 0.001), $^*P < 0.05$, $^{***}P < 0.001$, compared to control group, one-way ANOVA with Tukey's multiple comparisons test.

inflammation and to induce neural repair with minimal side effects. UA has been shown to prevent EAE by inhibiting Th17 cell differentiation when administered intraperitoneally before disease onset (14). We demonstrate in the present study that oral UA effectively reduces disease severity and improves clinical recovery at the onset, peak, and chronic phases of EAE and reduces numbers of both Th1 and Th17 cells. These effects, together with direct promotion of oligodendrocyte maturation and summarized in Fig. 9, provide evidence that UA has great value as an orally available agent with both antiinflammatory and neuroreparative capacities for MS.

An important reason for remyelination failure at the chronic stage of MS is that, despite OPC accumulation in CNS disease foci, their maturation process is halted (4, 6). Promoting OPC maturation into myelinating oligodendrocytes is therefore crucial for myelin repair. Neuroprotective approaches for CNS regeneration have thus far not been successful in clinical practice, and drugs that enhance remyelination are still not available for

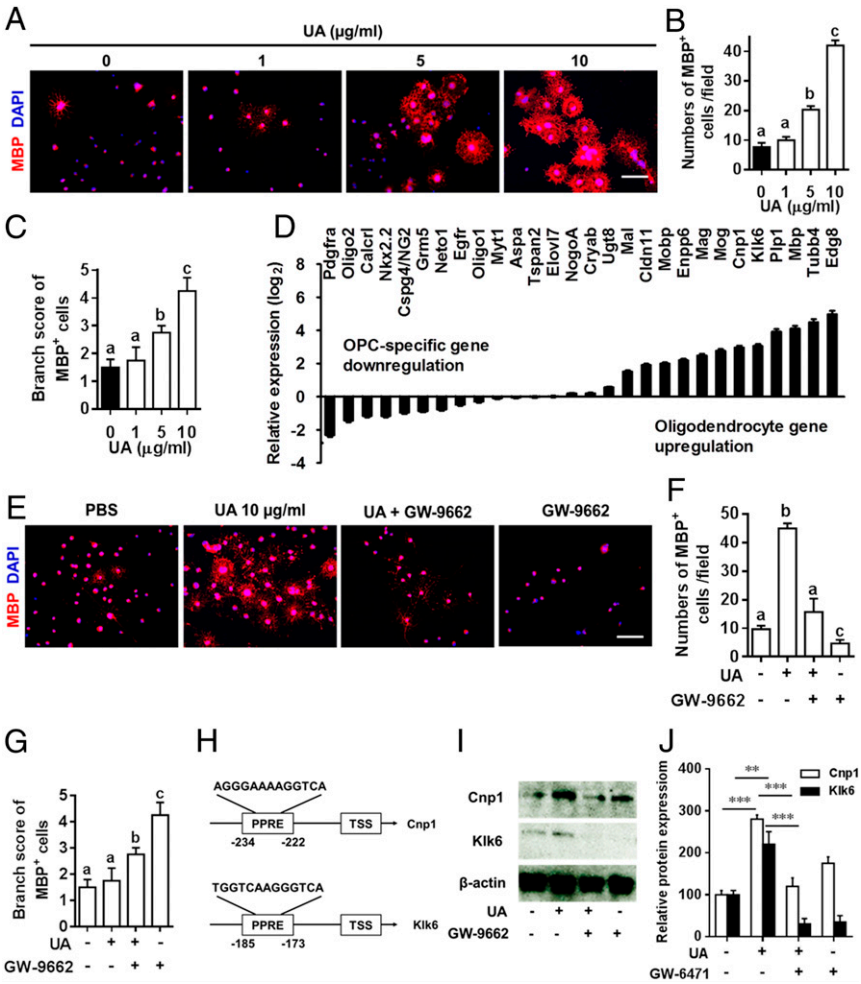

Fig. 8. UA directly induced OPC differentiation and myelin-related gene expression via PPARγ. (*A*) UA enhanced oligodendrocyte differentiation in primary OPC cultures. Primary OPCs, prepared from newborn C57BL/6J mouse brains, were cultured in differentiation medium with or without UA (1 to 10 μg/mL) for 5 to 7 d, followed by MBP immunofluorescence staining. Nuclei were stained with DAPI (blue). One of five representative experiments is shown. (Scale bar, 50 μm.) Quantitative analysis was performed for numbers (*B*) or branch score (*C*) of MBP$^+$ mature oligodendrocytes. (*D*) Expression of known genes associated with OPC maturation and myelination. Primary OPCs were cultured in differentiation medium for 5 d with or without UA (10 μg/mL), and OPC/oligodendrocyte-related genes were determined using Custom RT^2 Profiler PCR Array (Qiagen, Valencia, CA). (*E*) Primary OPCs were cultured in differentiation medium with UA (10 μg/mL) alone or pretreated for 30 min with GW-9662 (PPARγ-specific antagonist) before addition of UA, or GW-9662 (10 nM) alone, for 7 d followed by MBP immunofluorescence staining. Nuclei were stained with DAPI (blue). One of five representative experiments is shown. (Scale bar, 50 μm.) Quantitative analysis was performed for numbers (*F*) or branch score (*G*) of MBP$^+$ mature oligodendrocytes. (*H*) Position of PPREs in the promoters of mouse Cnp1 and Klk6. TSS: transcription start site. (*I*) Cnp1 and Klk6 expression in OPCs treated with UA and/or GW-9662 was detected by Western blot with specific antibodies. (*J*) Protein expression was standardized using β-actin as a sample loading control; quantification is presented in each panel. Data are shown as mean values ± SD (n = 5 to 6 per group) and are representative of three experiments. Groups designated by the same letter are not significantly different, while those with different letters are significantly different ($P < 0.05$ to 0.001). $^{**}P < 0.01$, $^{***}P < 0.001$, compared to control group, one-way ANOVA with Tukey's multiple comparisons test.

patients with demyelinating diseases. In the present study, the potential of UA as a promyelinating and neurorestorative therapy is clearly highlighted by several lines of evidence. First, when treatment was started at the chronic stage of EAE—when chronic demyelination, axonal damage, and neuron loss have already occurred—UA not only inhibited ongoing demyelination, but also promoted MBP production and increased numbers of myelinated axons and neuronal cells. Second, UA treatment enhanced remyelination and process extension of oligodendrocytes following both the cuprizone and LPC-induced demyelination of organotypic cerebellar slices, confirming that UA exerts a direct promyelination/remyelination effect, which is essential for regeneration of already damaged CNS tissues. Third, UA treatment drives primary OPCs to mature into oligodendrocytes in a dose-dependent manner in culture. Thus, whereas the in vivo effect of UA on remyelination and neural repair could result from a combination of both immunomodulation and a direct effect on CNS cells, results from organotypic slice cultures and primary OPCs confirm the capacity of UA to promote remyelination in addition to, or independent of, immunomodulation. This effect, together with its effect on neuronal protection (14), provides a solid basis to consider UA for neuroreparative therapy.

Loss of neurotrophic factors has been implicated in the pathogenesis of MS, and increasing their levels and/or maintaining their physiological levels in the CNS is beneficial for MS patients (23, 29, 30). However, attempts for clinical application of neurotrophic factors were limited because of poor penetration

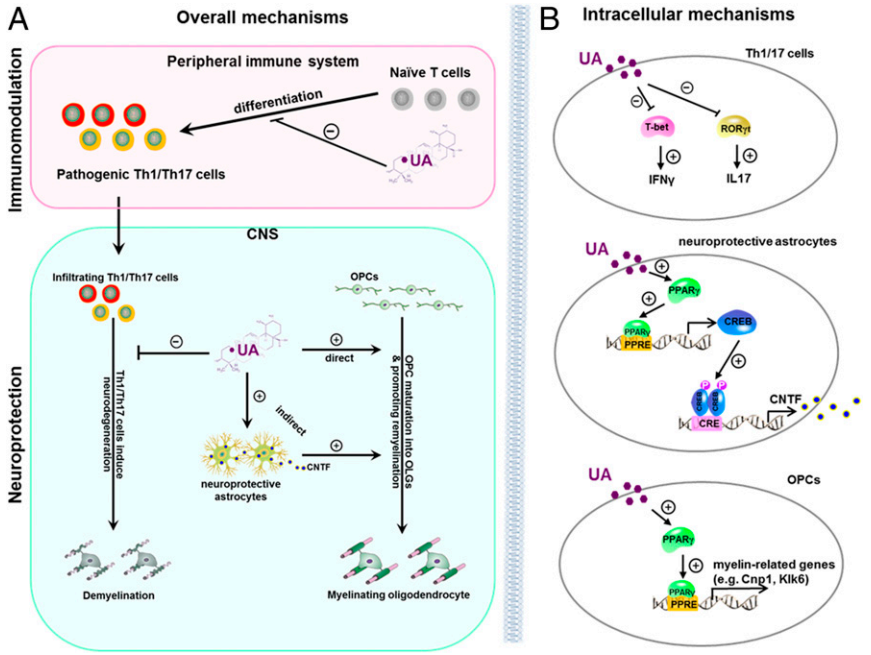

Fig. 9. Model of UA-mediated immunomodulation and neuroregeneration effects in EAE. (*A*) Extracellular effects of UA treatment in the periphery and CNS. In the periphery, UA inhibits Th1/Th17 cell differentiation and decreases Th1/Th17 cell infiltration in the CNS. In the CNS, UA reduces inflammation and demyelination and promotes OPC maturation and remyelination via direct and indirect mechanisms. (*B*) Intracellular mechanisms of UA effects on Th1/Th17 cells, astrocytes, and OPCs. During T cell differentiation, UA suppresses IFN-γ and IL-17 production by antagonizing the functions of T-bet and RORγt. In astrocytes, UA activates PPARγ, which was recruited to PPRE of CREB promoter and leads to the transcription of CREB. CREB then binds to the CRE site of CNTF promoter to promote expression of CNTF. Activated astrocytes under UA treatment release CNTF, an important neurotrophic factor for OPC differentiation with strong promyelination effect. UA induces CNTF expression in astrocytes that favor the beneficial outcome of reactive astrogliosis and are thus considered neuroprotective. Furthermore, UA directly induces OPC differentiation by activated PPARγ, which binds to PPRE of promoters and leads to expression of different myelin-related genes such as Cnp1 and Klk6.

into the CNS and low bioavailability (31). Thus, drugs that have the ability to induce expression of neurotrophic factors and restore their levels in the CNS would be a feasible approach to overcome such issues. Our current study clearly shows that in astrocytes UA robustly up-regulates CNTF, a strong promyelinating neurotrophic factor that exhibits beneficial effects in EAE (23, 32). Importantly, while the supernatants of UA-treated astrocytes supported maturation of MBP^+ oligodendrocytes, the effect was specifically abolished by CNTF-neutralizing antibodies. We therefore conclude that UA induces CNTF production by astrocytes, thus promoting remyelination. The contribution of other less-induced neurotrophic factors may also be important, and this would be worthy of further investigations.

UA has been shown to be a potent agonist of PPARγ (19); we therefore tested the involvement of this pathway in the effect of UA on astrocytes. Indeed, UA induced PPAR activation in astrocytes, and inhibition of PPARγ significantly suppressed UA-induced CNTF production by these cells. As a key nuclear receptor, PPARγ/RXR (retinoid X receptor) signaling has been identified as an important regulator of remyelination (33, 34). In elucidating how the PPARγ pathway regulates the transcription of CNTF in astrocytes, we observed that UA-induced CNTF synthesis was markedly diminished by knockdown of CREB in cultured astrocytes. Furthermore, UA failed to drive expression of the CREB promoter containing a mutated PPRE site, indicating a crucial role for PPARs in the transcription of CREB activated by UA. Taken together, these findings demonstrate that UA enhances the expression of astrocyte-derived CNTF through PPARγ and CREB signal pathways.

In addition to the indirect mechanisms through astrocyte-derived CNTF, we provide compelling evidence indicating that UA directly induced myelin-related gene expression and OPC maturation via PPARγ signaling. PPARγ agonists have been shown to protect OPCs by preserving their integrity and favoring their differentiation into myelin-forming cells, and they may promote recovery from demyelination by direct effects on oligodendrocytes (20, 35); our results indicate that this is also the case for UA treatment. Although UA-induced up-regulation of the oligodendrocyte-related molecules Cnp1 and Klk6 is PPARγ dependent, the molecular mechanism of UA-induced down-regulation of OPC-specific molecules, e.g., Olig2, Nkx2.2, NG2, and PDGFRα, is still unclear. Given that these OPC-related genes have no PPREs in their promoter, UA may modulate expression of these genes via PPARγ-independent signaling. These mechanisms are not completely understood and continue to be a topic of active investigation.

Recent reports using high-throughput screening have identified a number of compounds that enhance remyelination (36–39). However, the clinical potential of some compounds is limited by deleterious side effects and/or their action on off-target receptors. Continued screening of novel small molecule compounds is clearly an unmet need. As a natural compound found ubiquitously in plants and human diets, UA has low toxicity and is well tolerated when administered orally in both humans and rodents (8, 9, 40). UA has been identified as an active component in many medicinal herbs; it has long been used in clinical practice in Asian countries and is inexpensive (40). In the present study, the UA dose that proved effective for EAE treatment (25 mg/kg/d) is ~350 times lower than the dose showing acute toxicity (LD_{50} = 8,330 mg/kg) (41). Furthermore, UA is currently undergoing clinical trials to evaluate safety in patients with tumors (42–44); preliminary results demonstrated that UA is safe and has beneficial therapeutic effects in select patients (40), suggesting that UA would be safe as MS treatment. Importantly, analysis of the distribution of UA orally administered to mice for 4 or 8 wk has shown that this lipophilic compound crosses the blood–brain barrier and is sequestered in the brain parenchyma (45), giving UA the great advantage of being able to exert effects directly on CNS cells.

Taken together, our findings provide important insights into the neural repair capacities of UA through both immunomodulation and oligodendrocyte maturation in the chronic phase of experimental models of MS. We also provide detailed intracellular mechanisms responsible for UA action in the development of Th1/Th17 cells, astrocytes, and OPCs (diagram in Fig. 9*B*). These studies, together with the excellent safety record

of UA, its low cost, and oral route of administration, pave the way for clinical applications in the chronic stage of MS, for which there is currently no effective therapy.

Materials and Methods

A complete description of the methods and associated references are in *SI Appendix, Materials and Methods*. The EAE and cuprizone-induced demyelination model were treated with UA. All experimental procedures and protocols of mice were approved by the Institutional Animal Care and Use Committee of Thomas Jefferson University and were carried out in accordance with the approved institutional guidelines and regulations. C57BL/6J mice (8 to 10 wk of age) and PPARγ$^{+/-}$ mice (C57BL/6J background) were purchased from Jackson Laboratory (Bar Harbor, ME). The reagents and experimental procedure for histopathological examination, preparation of infiltrating MNCs from the CNS, cytokine measurement by ELISA, flow cytometry, molecular docking, organotypic slice cultures, isolation of primary mouse astrocytes and OPCs, electron microscopy, immunofluorescence, transient transfection and luciferase reporter assay, Western blot analysis, real-time RT-PCR, and other experiments mentioned in this paper are discussed in *SI Appendix, Materials and Methods*.

Data Availability. The authors confirm that all data supporting the findings of this study are included in the main text and *SI Appendix*.

ACKNOWLEDGMENTS. This study was supported by the NIH, USA (Grants NS099594 and AI135601). Y.Z. and X.L. are partly supported by the Chinese National Natural Science Foundation (Grants 81771345 and 31970771) and the Open Fund of Shanxi Key Laboratory of Inflammatory Neurodegenerative Diseases (Grant KF2019001). We thank Ms. Katherine Regan and Ms. Pamela Walter for editorial assistance.

1. M. Tintore, A. Vidal-Jordana, J. Sastre-Garriga, Treatment of multiple sclerosis: Success from bench to bedside. *Nat. Rev. Neurol.* **15**, 53–58 (2019).
2. J. Correale, M. I. Gaitán, M. C. Ysrraelit, M. P. Fiol, Progressive multiple sclerosis: From pathogenic mechanisms to treatment. *Brain* **140**, 527–546 (2017).
3. N. Cunniffe, A. Coles, Promoting remyelination in multiple sclerosis. *J. Neurol.*, 10.1007/s00415-019-09421-x (2019).
4. M. Stangel, T. Kuhlmann, P. M. Matthews, T. J. Kilpatrick, Achievements and obstacles of remyelinating therapies in multiple sclerosis. *Nat. Rev. Neurol.* **13**, 742–754 (2017).
5. S. A. Goldman, M. Nedergaard, M. S. Windrem, Glial progenitor cell-based treatment and modeling of neurological disease. *Science* **338**, 491–495 (2012).
6. R. J. Franklin, Regenerative medicines for remyelination: From aspiration to reality. *Cell Stem Cell* **16**, 576–577 (2015).
7. H. Hussain *et al*., Ursolic acid derivatives for pharmaceutical use: A patent review (2012-2016). *Expert Opin. Ther. Pat.* **27**, 1061–1072 (2017).
8. S. Y. Lee, Y. J. Kim, S. O. Chung, S. U. Park, Recent studies on ursolic acid and its biological and pharmacological activity. *EXCLI J.* **15**, 221–228 (2016).
9. D. Kashyap, H. S. Tuli, A. K. Sharma, Ursolic acid (UA): A metabolite with promising therapeutic potential. *Life Sci.* **146**, 201–213 (2016).
10. H. Mortiboys, J. Aasly, O. Bandmann, Ursocholanic acid rescues mitochondrial function in common forms of familial Parkinson's disease. *Brain* **136**, 3038–3050 (2013).
11. E. Y. Kim *et al*., Ursolic acid facilitates apoptosis in rheumatoid arthritis synovial fibroblasts by inducing SP1-mediated Noxa expression and proteasomal degradation of Mcl-1. *FASEB J.* **32**, fj201800425R (2018).
12. A. Alqahtani *et al*., The pentacyclic triterpenoids in herbal medicines and their pharmacological activities in diabetes and diabetic complications. *Curr. Med. Chem.* **20**, 908–931 (2013).
13. H. Xu *et al*., Low and high doses of ursolic acid ameliorate experimental autoimmune myasthenia gravis through different pathways. *J. Neuroimmunol.* **281**, 61–67 (2015).
14. T. Xu *et al*., Ursolic acid suppresses interleukin-17 (IL-17) production by selectively antagonizing the function of RORgamma t protein. *J. Biol. Chem.* **286**, 22707–22710 (2011).
15. A. B. Ramos-Hryb, F. L. Pazini, M. P. Kaster, A. L. S. Rodrigues. Therapeutic potential of ursolic acid to manage neurodegenerative and psychiatric diseases. *CNS Drugs* **31**, 1029–1041 (2017).
16. P. G. Bannerman *et al*., Motor neuron pathology in experimental autoimmune encephalomyelitis: Studies in THY1-YFP transgenic mice. *Brain* **128**, 1877–1886 (2005).
17. Y. H. Shih, Y. C. Chein, J. Y. Wang, Y. S. Fu, Ursolic acid protects hippocampal neurons against kainate-induced excitotoxicity in rats. *Neurosci. Lett.* **362**, 136–140 (2004).
18. K. Wilkinson, J. D. Boyd, M. Glicksman, K. J. Moore, J. El Khoury, A high content drug screen identifies ursolic acid as an inhibitor of amyloid beta protein interactions with its receptor CD36. *J. Biol. Chem.* **286**, 34914–34922 (2011).
19. S. H. Kim, J. H. Hong, Y. C. Lee, Ursolic acid, a potential PPARγ agonist, suppresses ovalbumin-induced airway inflammation and Penh by down-regulating IL-5, IL-13, and IL-17 in a mouse model of allergic asthma. *Eur. J. Pharmacol.* **701**, 131–143 (2013).
20. W. Cai *et al*., Peroxisome proliferator-activated receptor γ (PPARγ): A master gatekeeper in CNS injury and repair. *Prog. Neurobiol.* **163–164**, 27–58 (2018).
21. J. Praet, C. Guglielmetti, Z. Berneman, A. Van der Linden, P. Ponsaerts, Cellular and molecular neuropathology of the cuprizone mouse model: Clinical relevance for multiple sclerosis. *Neurosci. Biobehav. Rev.* **47**, 485–505 (2014).
22. A. A. Jarjour, H. Zhang, N. Bauer, C. Ffrench-Constant, A. Williams, In vitro modeling of central nervous system myelination and remyelination. *Glia* **60**, 1–12 (2012).
23. R. A. Linker *et al*., CNTF is a major protective factor in demyelinating CNS disease: A neurotrophic cytokine as modulator in neuroinflammation. *Nat. Med.* **8**, 620–624 (2002).
24. K. A. Stöckli *et al*., Regional distribution, developmental changes, and cellular localization of CNTF-mRNA and protein in the rat brain. *J. Cell Biol.* **115**, 447–459 (1991).
25. Y. Yan *et al*., CNS-specific therapy for ongoing EAE by silencing IL-17 pathway in astrocytes. *Mol. Ther.* **20**, 1338–1348 (2012).
26. J. B. Kim, H. M. Wright, M. Wright, B. M. Spiegelman, ADD1/SREBP1 activates PPARgamma through the production of endogenous ligand. *Proc. Natl. Acad. Sci. U.S.A.* **95**, 4333–4337 (1998).
27. A. Roy *et al*., Regulation of cyclic AMP response element binding and hippocampal plasticity-related genes by peroxisome proliferator-activated receptor α. *Cell Rep.* **4**, 724–737 (2013).
28. M. K. Paintlia, A. S. Paintlia, A. K. Singh, I. Singh, S-nitrosoglutathione induces ciliary neurotrophic factor expression in astrocytes, which has implications to protect the central nervous system under pathological conditions. *J. Biol. Chem.* **288**, 3831–3843 (2013).
29. R. Giess *et al*., Association of a null mutation in the CNTF gene with early onset of multiple sclerosis. *Arch. Neurol.* **59**, 407–409 (2002).
30. R. Brambilla, The contribution of astrocytes to the neuroinflammatory response in multiple sclerosis and experimental autoimmune encephalomyelitis. *Acta Neuropathol.* **137**, 757–783 (2019).
31. D. F. Emerich, C. G. Thanos, Intracompartmental delivery of CNTF as therapy for Huntington's disease and retinitis pigmentosa. *Curr. Gene Ther.* **6**, 147–159 (2006).
32. T. Kuhlmann *et al*., Continued administration of ciliary neurotrophic factor protects mice from inflammatory pathology in experimental autoimmune encephalomyelitis. *Am. J. Pathol.* **169**, 584–598 (2006).
33. K. A. Hanafy, J. A. Sloane, Regulation of remyelination in multiple sclerosis. *FEBS Lett.* **585**, 3821–3828 (2011).
34. J. K. Huang *et al*., Retinoid X receptor gamma signaling accelerates CNS remyelination. *Nat. Neurosci.* **14**, 45–53 (2011).
35. A. Bernardo, D. Bianchi, V. Magnaghi, L. Minghetti, Peroxisome proliferator-activated receptor-gamma agonists promote differentiation and antioxidant defenses of oligodendrocyte progenitor cells. *J. Neuropathol. Exp. Neurol.* **68**, 797–808 (2009).
36. Z. Hubler *et al*., Accumulation of 8,9-unsaturated sterols drives oligodendrocyte formation and remyelination. *Nature* **560**, 372–376 (2018).
37. F. Luo *et al*., Modulation of proteoglycan receptor PTPσ enhances MMP-2 activity to promote recovery from multiple sclerosis. *Nat. Commun.* **9**, 4126 (2018).
38. F. Mei *et al*., Micropillar arrays as a high-throughput screening platform for therapeutics in multiple sclerosis. *Nat. Med.* **20**, 954–960 (2014).
39. F. J. Najm *et al*., Drug-based modulation of endogenous stem cells promotes functional remyelination in vivo. *Nature* **522**, 216–220 (2015).
40. Ł. Woźniak, S. Skąpska, K. Marszałek, Ursolic acid: A pentacyclic triterpenoid with a wide spectrum of pharmacological activities. *Molecules* **20**, 20614–20641 (2015).
41. A. W. Lee *et al*., Ursolic acid induces allograft inflammatory factor-1 expression via a nitric oxide-related mechanism and increases neovascularization. *J. Agric. Food Chem.* **58**, 12941–12949 (2010).
42. Z. Zhu *et al*., A phase I pharmacokinetic study of ursolic acid nanoliposomes in healthy volunteers and patients with advanced solid tumors. *Int. J. Nanomedicine* **8**, 129–136 (2013).
43. X. H. Wang *et al*., Evaluation of toxicity and single-dose pharmacokinetics of intravenous ursolic acid liposomes in healthy adult volunteers and patients with advanced solid tumors. *Expert Opin. Drug Metab. Toxicol.* **9**, 117–125 (2013).
44. Z. Qian *et al*., A phase I trial to evaluate the multiple-dose safety and antitumor activity of ursolic acid liposomes in subjects with advanced solid tumors. *BioMed Res. Int.* **2015**, 809714 (2015).
45. M. C. Yin, M. C. Lin, M. C. Mong, C. Y. Lin, Bioavailability, distribution, and antioxidative effects of selected triterpenes in mice. *J. Agric. Food Chem.* **60**, 7697–7701 (2012).